A bioinspired microfluidic model of liquid plug-induced mechanical airway injury

Joseph W. Song,[1] Jungwook Paek,[1] Kyu-Tae Park,[1] Jeongyun Seo,[1,2] and Dongeun Huh[1,2,3,a)]

[1]*Department of Bioengineering, University of Pennsylvania, Philadelphia, Pennsylvania 19104, USA*
[2]*NSF Science and Technology Center for Engineering Mechanobiology, University of Pennsylvania, Philadelphia, Pennsylvania 19104, USA*
[3]*Institute for Regenerative Medicine, Perelman School of Medicine, University of Pennsylvania, Philadelphia, Pennsylvania 19104, USA*

(Received 1 March 2018; accepted 7 May 2018; published online 29 May 2018)

Occlusion of distal airways due to mucus plugs is a key pathological feature common to a wide variety of obstructive pulmonary diseases. Breathing-induced movement of airway mucus plugs along the respiratory tract has been shown to generate abnormally large mechanical stresses, acting as an insult that can incite acute injury to the airway epithelium. Here, we describe a unique microengineering strategy to model this pathophysiological process using a bioinspired microfluidic device. Our system combines an air-liquid interface culture of primary human small airway epithelial cells with a microengineered biomimetic platform to replicate the process of mucus exudation induced by airway constriction that leads to the formation of mucus plugs across the airway lumen. Specifically, we constructed a compartmentalized three-dimensional (3D) microfluidic device in which extracellular matrix hydrogel scaffolds reminiscent of airway stroma were compressed to discharge fluid into the airway compartment and form liquid plugs. We demonstrated that this plug formation process and subsequent movement of liquid plugs through the airway channel can be regulated in a precisely controlled manner. Furthermore, we examined the detrimental effect of plug propagation on the airway epithelium to simulate acute epithelial injury during airway closure. Our system allows for a novel biomimetic approach to modeling a complex and dynamic biophysical microenvironment of diseased human airways and may serve as an enabling platform for mechanistic investigation of key disease processes that drive the progression and exacerbation of obstructive pulmonary diseases. *Published by AIP Publishing.*
https://doi.org/10.1063/1.5027385

INTRODUCTION

The respiratory tract in mammalian lungs is covered with a slippery aqueous secretion produced by secretory cells in the airway epithelium and submucosal glands. This thin liquid lining plays a crucial role in organ homeostasis by providing a protective barrier against inhaled foreign insults and also functioning as a biological surfactant to mitigate mechanical stresses generated by dynamic tissue deformation and fluid flow in the respiratory system.[1] Studies have shown that development and progression of various pulmonary disorders are associated with abnormal changes in the airway surface liquid. For example, in obstructive lung diseases such as chronic obstructive pulmonary disease (COPD)[2,3] and asthma,[4] frequent bronchoconstriction or irreversible constrictive airway remodeling induces discharge and excessive build-up of mucus and cellular exudates in the airway lumen, eventually leading to the blockage of air

a)Author to whom correspondence should be addressed: huhd@seas.upenn.edu

passages [Fig. 1(a)].[5] Mucus hyper-secretion from goblet cells commonly associated with many of these diseases also contributes to impaired liquid balance in the respiratory tract and the formation of mucus plugs that occlude the airway lumen.[5]

Importantly, these airway liquid plugs not only impede airflow and gas exchange in the lung but can also generate abnormal mechanical forces that may be detrimental to the airway epithelium. Computation studies have shown that the movement of mucus plugs induced by breathing [Fig. 1(b)] gives rise to large gradients of pressure and shear stress on the airway wall.[6–11] Researchers have also suggested the deleterious potential of this abnormal mechanical microenvironment by demonstrating significantly reduced cell viability due to the passage of air bubbles over the surface of airway epithelial cells cultured in submerged conditions.[12–14] While these early studies have improved our understanding of the pathophysiological significance of pulmonary liquid plugs, further progress in this area has been greatly hampered by the technical challenges associated with emulating complex dynamics of plug formation and movement in a physiologically relevant and organ-specific model system.

In an attempt to suggest potential solutions to this problem, here, we present a biomimetic microengineering strategy to recapitulate the pathophysiological process of airway closure due to mucus plugs and to simulate and analyze cellular responses to plug propagation. Our work builds upon recent advances in the development of microengineered platforms to investigate physics and biological effects of liquid plugs in the human lungs,[15–21] especially the work of the Takayama group that demonstrated a microfluidic airway model for the study of airway reopening-induced acute lung injury.[16,17,19,20] By combining multi-layered microdevice architecture with mechanical manipulation of 3D extracellular matrix (ECM) hydrogel constructs, this paper introduces a new method for reconstituting the dynamic process of airway mucus occlusion in a more physiologically relevant manner. Specifically, we created a microfluidic platform

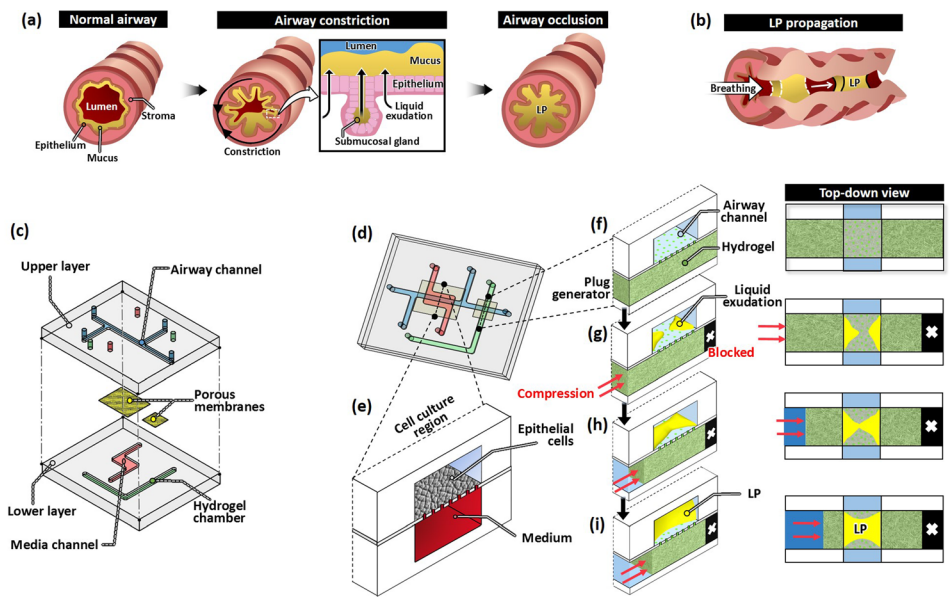

FIG. 1. Microengineered airway model. (a) In many obstructive lung diseases, compressive deformation of pulmonary airways due to airway constriction results in exudation of mucus and interstitial fluid from the sub-epithelial compartment into the airway lumen, forming liquid plugs that occlude the air passage. (b) Pressure drop due to breathing prompts these liquid plugs to propagate through the airways. LP stands for liquid plug. [(c) and (d)] A microphysiological airway-on-a-chip designed to mimic this process of airway mucus plugging and plug propagation is constructed by bonding two layers of microfabricated channels and semipermeable membrane supports. (e) In the cell culture region, primary human airway epithelial cells are cultured on the membrane to form differentiated pulmonary epithelial tissue. (f) To simulate the formation of mucus plugs due to airway constriction, collagen hydrogel is formed in the hydrogel chamber in the lower channel layer. (g) Hydraulic pressure is applied to the hydrogel scaffold while the outlet of the hydrogel chamber is blocked. The applied compression induces exudation of liquid in the hydrogel into the airway channel. [(h) and (i)] The fluid leakage continues and eventually forms a liquid plug in the airway channel.

capable of mimicking mucus exudation induced by mechanical compression of the sub-epithelial stroma during pathological airway constriction to form microscopic liquid plugs. We also integrated this biomimetic plug generator with a compartmentalized 3D microchannel system to demonstrate microfluidic culture and differentiation of primary human small airway epithelial cells (SAECs) at the air-liquid interface (ALI) and their exposure to moving plugs. Using this integrated airway-on-a-chip model, we show that the propagation of liquid plugs through the airway compartment can induce (i) significant epithelial injury, (ii) reorganization of cytoskeletal architecture, and (iii) activation of pro-inflammatory signaling pathways in a dose-dependent manner.

DEVICE DESIGN, CONSTRUCTION, AND OPERATION

Our airway-on-a-chip model is constructed using two elastomeric layers of microfabricated channels made out of poly(dimethylsiloxane) (PDMS). The airway channel in the upper layer is bonded to the media channel and the hydrogel chamber in the lower layer with two pieces of semipermeable membrane support sandwiched in between [Fig. 1(c)]. Once assembled, this multilayered device provides individually addressable yet interconnected fluidic compartments for growth and differentiation of airway epithelial cells, as well as for the production of liquid plugs [Fig. 1(d)]. To form the airway epithelial tissue, primary human SAECs are seeded into the cell culture region of the airway channel and grown on a porous membrane to confluence, after which the cells are cultured at the air-liquid interface (ALI) for differentiation [Fig. 1(e)].

Another key component of our device is a biomimetic plug generator connected to the cell culture region via a common airway channel. Our method of plug formation is based on mechanical compression of a fully hydrated ECM hydrogel in confinement. First, a small volume of ECM hydrogel precursor solution is injected into the hydrogel chamber in the lower layer of the device and solidified to form a 3D hydrogel construct that represents the stromal connective tissue in the airway [Fig. 1(f)]. In the next step, the outlet of the hydrogel chamber is blocked [Fig. 1(g)], and an aqueous buffer solution is pumped into the chamber to mechanically compress the hydrogel and to mimic compressive forces experienced by the stromal tissue during airway constriction or pathological tissue remodeling [Fig. 1(h)]. As a result of compression, the liquid contained in the hydrogel begins to seep through the pores of the permeable membrane into the airway channel. Continuous fluid leakage due to sustained compression eventually leads to the formation of a liquid plug across the airway channel [Fig. 1(i)]. This process is reminiscent of airway constriction-induced exudation of mucus and interstitial fluid from the sub-epithelial stromal compartment into the airway lumen in obstructive pulmonary diseases.[5] Liquid plugs generated in this manner are then propelled by compressed air down the airway channel to the cell culture region lined with airway epithelial cells.

METHODS

Fabrication of the microdevice

The upper and lower PDMS slabs containing microchannel features were fabricated using standard soft lithography techniques. Briefly, PDMS (Sylgard 184, Dow Corning) base was mixed thoroughly with a curing agent at a weight ratio of 10:1 (base:curing agent) and poured onto 3D-printed channel molds (ProtoLab). The cross-sectional dimensions of the airway channel and the hydrogel chamber were 1 mm (width) $\times$ 500 μm (height). After degassing, PDMS was fully cured in an oven maintained at 65 °C. The hardened PDMS was then removed from the molds, and fluidic access ports were punched through the slabs. To bond the channel layers, they were first stamped against a thin layer of uncured PDMS prepared by spin-coating at 1500 rpm for 5 min. Following this step, two pieces of permeable membrane were placed at their desired locations on the PDMS stamped upper channel slab and then bonded to the other layer. The assembled device was incubated at 65 °C to fully cure the PDMS adhesive layer. In our study, two types of optically transparent semipermeable membranes were used; polyester

membranes with 0.4 μm pores (Costar 3450) for the cell culture region and polyester membranes with 3 μm pores (Costar 3452) for the plug generator.

Microfluidic cell culture

To form the airway epithelium in our model, we used primary human small airway epithelial cells (SAECs) (CC-2547, Lonza) along with their growth (CC-3118, Lonza) and differentiation (CC-4539, Lonza) media. Before use in microchannels, the cells were maintained in complete growth media and cultured in 25-cm^2 flasks according to the manufacturer's protocols. Cells were used for microfluidic culture after the first or second subculture. For microfluidic cell culture, the fully assembled device was sterilized by exposing it to ultraviolet (UV) light (Electro-lite ELC-500) for at least 30 min. Subsequently, the airway channel in the upper layer was filled and incubated with a fibronectin solution [0.1 mg/ml in phosphate-buffered saline (PBS)] (Corning-356008) to generate ECM coating on the membrane surface for cell attachment. After 2-h incubation, the channel was washed with PBS, filled with the culture medium, and incubated in a cell culture incubator at 37 °C and 5% CO_2 for 2 h. As the first step of cell seeding, trypsinized SAECs were suspended in their growth medium at a concentration of 2×10^6 cells/ml, and the cell suspension was injected into the airway channel. Immediately after seeding, the access ports were blocked to completely stop fluid flow and allow the seeded cells to settle to the membrane surface and attach. Once firm attachment was established, the media channel in the lower layer was filled with the culture medium as well. During submerged culture, culture media in the airway and media channels were replenished daily for 3 days until the formation of a confluent monolayer on the membrane surface. Prior to the initiation of ALI culture, the growth medium used for submerged culture in both channels was switched to differentiation medium. After 24 h of incubation, the medium in the airway channel was gently aspirated to expose the epithelial monolayer to air. During ALI culture, the cells were fed from their basolateral side with freshly delivered differentiation medium in the media channel. ALI culture was conducted for 5 days.

Generation and propagation of liquid plugs

Rat tail collagen type I (Corning-354236) was used to create an ECM hydrogel scaffold for the production of liquid plugs. A collagen precursor solution (2 mg/ml) was injected into the hydrogel chamber and polymerized in a cell culture incubator for 30 min. Generation of liquid plugs was accomplished by first blocking the outlet of the hydrogel chamber and then injecting Dulbecco's PBS (DPBS) solution into the chamber using a computer-controlled syringe pump (Chemyx) at a volumetric flow rate of 1 ml/min, during which liquid in the compressed hydrogel leaked into the airway channel and accumulated on the membrane and channel surfaces. Once a liquid plug was formed, it was pushed down the airway channel to the cell culture region by injecting compressed air at 0.05 ml/min to generate airflow through the channel. This process was repeated as needed for exposure of the airway epithelium to multiple passages of liquid plugs. Two frequencies of plug propagation (5 and 10 plugs at 1 propagation/min) were tested in our study to investigate dose-dependent cellular responses.

Viability assay

After mechanical stimulation with liquid plugs, the airway channel was filled with the culture medium and incubated at 37 °C and 5% CO_2 for 30 min. This resting step was designed to permit healing and recovery of transient cellular injury immediately after plug propagation and to identify permanently damaged cells for our analysis. Subsequently, a mixture of calcein AM and ethidium homodimer-1 (2 μM and 4 μM in the culture medium, respectively) was introduced into the airway channel and incubated at 37 °C for 20 min. Following this step, the airway channel was washed with DPBS 3 times and inspected using an inverted epi-fluorescence microscope (Zeiss Axio Observer). For quantitative analysis of cellular viability, we averaged

the fraction of live and dead cells over at least three different regions of interest in any given device. Data were collected from three independent experiments.

Immunostaining and quantification

For immunostaining, SAECs in microfluidic devices were fixed in 4% paraformaldehyde for 10 min, washed with DPBS, and permeabilized with 0.25% Triton X-100 for 10 min. Subsequently, a blocking step was performed using 3% bovine serum albumin (BSA) for 1 h at room temperature (RT). For imaging epithelial tight junctions, the cells were incubated with ZO-1 antibody (33-9100, ThermoFisher) overnight at 4 °C and then the secondary antibody (A-11005, ThermoFisher) for 1 h at RT with rinsing steps in between. Visualization of the actin cytoskeleton was achieved by treating the cells with Alexa Fluor 488 conjugated phalloidin (Life Technologies) for 30 min. Finally, Hoechst 33342 (ThermoFisher) was used for nuclear staining. Using the Zen software (Zeiss Microscopy), the mean fluorescence intensity of F-actin staining was calculated from three independent experiments and used as quantitative metrics for assessment of plug propagation-induced alterations in intracellular architecture. We also conducted quantitative analysis using the Ridge Detection Plugin in ImageJ[22] to evaluate the average number of stress fibers under different loading conditions.

To stain nuclear factor (NF)-κB, the device was incubated with the NF-κB antibody (ab16502, Abcam) overnight at 4 °C followed by treatment with the secondary antibody (ab150077, Abcam) for 1 h at RT. The cells were stained 24 h after their exposure to plug propagation to allow sufficient time for activation of NF-κB. In this analysis, we measured nuclear translocation of NF-κB by evaluating the ratio of average fluorescence intensity in the nuclei to the cytoplasm. Immunofluorescence images used in our analysis were taken from three independent experiments.

Statistical analysis

Statistical significance of the obtained data was evaluated by a two-tailed t-test. Data were presented as mean ± SD.

RESULTS AND DISCUSSION

Liquid plug generation

The main novelty of our microphysiological airway model lies in its ability to recapitulate mucus plugging due to constrictive tissue deformation in its *in vivo* counterparts. The initial phase of our study focused on demonstrating this key feature and characterizing the process of plug formation in a quantitative manner. As described above, our method relies on controlled mechanical compression of 3D matrices that mimic stromal tissue in the airway. The compartmentalized design of our device made it possible to generate ECM hydrogel structures required for this biomimetic actuation. During injection and gelation of collagen solution in the hydrogel chamber, the intervening porous membrane acted as a physical barrier to effectively prevent unwanted leakage of the solution into the airway channel, permitting the formation of the spatially confined 3D collagen hydrogel in our device [Fig. 2(a)]. When the hydrogel chamber was pressurized by injecting a buffer solution while the outlet was blocked, the liquid was observed to seep through the membrane at the junction between the hydrogel chamber and the airway channel as shown in Fig. 2(b). The leaked liquid formed droplets that preferentially accumulated and extended along the sidewalls of the airway channel, presumably due to greater surface adhesive forces at the corners of the channel. Continued application of hydraulic compression to the collagen hydrogel caused a progressive increase in the volume of the liquid droplets over time, eventually leading to droplet merging and resultant formation of a liquid plug [Figs. 2(c) and 2(d)].

Our method also provided a means to precisely control plug length. The length of a liquid plug, which is defined by the shortest distance between the front and rear menisci of the plug, was measured to be approximately 1 mm when compression was applied for the minimum

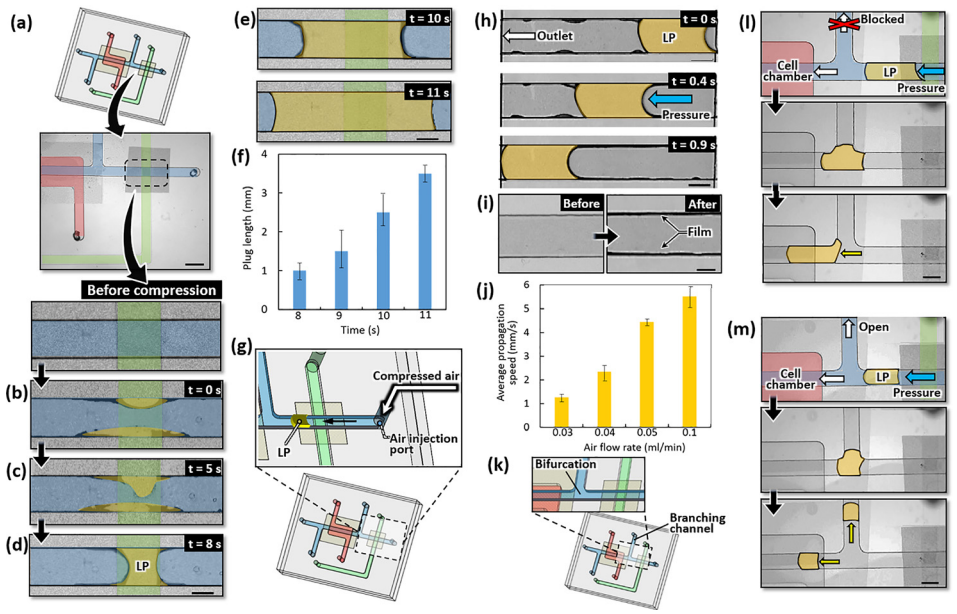

FIG. 2. Dynamics of liquid plug formation and propagation in the airway-on-a-chip. (a) The biomimetic plug generator is shown by a dotted rectangle in the micrograph of our fully assembled airway-on-a-chip device (upper image). The zoomed-in view of this region (lower image) shows the airway channel in the upper layer (pseudo-colored blue) and the collagen hydrogel-containing chamber in the lower layer (pseudo-colored green). Scale bars, 2 mm (upper micrograph) and 500 μm (lower micrograph). [(b)–(d)] As the collagen hydrogel is compressed, liquid (pseudo-colored yellow) leaks through the membrane pores and accumulates in the airway channel. Within 8 s, the accumulating liquid forms a plug that blocks the channel. Scale bar, 500 μm. LP stands for liquid plug. [(e) and (f)] The length of plugs can be controlled by varying the duration of hydrogel compression. Liquid plugs are pseudo-colored yellow. Scale bar, 500 μm. Data in (f) show mean ± SD with $n = 3$. (g) The propagation of liquid plugs is achieved by injecting compressed air into the airway channel through an injection port. (h) The injected air pushes a liquid plug through the airway channel. Scale bar, 650 μm. Liquid plugs are pseudo-colored yellow. (i) Propagation liquid plugs form thin liquid lining on the surface of the airway channel. The liquid film appears as dark bands along the sidewalls of the channel in the micrograph (right). Scale bar, 500 μm. (j) Propagation speed can be regulated by the flow rate of compressed air injected into the airway channel. Data show mean ± SD with $n = 3$ for a plug length of approximately 2 mm. (k) A branching channel in the upper layer creates a channel bifurcation. (l) When the branching channel is closed off, a liquid plug traveling down the channel is lodged briefly at the bifurcation but passes through and moves towards the cell culture region. Liquid plugs are pseudo-colored yellow. Scale bar, 1 mm. (m) when the branching channel is open, the lodged plug at the channel bifurcation is split into two daughter plugs. Scale bar, 1 mm.

amount for time (8 s) required for plug formation. As shown in Figs. 2(e) and 2(f), however, this length was readily adjustable by varying the duration of pressure loading in the hydrogel chamber. For example, pressure application for 10 and 11 s resulted in a plug length of 2.5 and 3.5 mm, respectively. Interestingly, this increase in plug length was accompanied by concomitant reduction in the curvature of both the front and rear menisci, reflecting increased internal pressure in longer liquid plugs. Considering that the length of airway closure during plug-induced airway obstruction is highly variable,[23] these results support the capability of our model to mimic the physiological context of airway mucus occlusion in a more realistic manner.

Propagation of liquid plugs

Next, we examined the movement of liquid plugs from the plug generator to the cell culture region of the airway channel. Plug propagation in our device was induced by flowing compressed air into the air injection port [Fig. 2(g)]. Importantly, the flow rate of injected air during this procedure was tightly regulated by a computer-controlled pump to match the physiological range of plug propagation velocity (1–10 mm/s) estimated for respiratory and terminal bronchioles in the human lung at normal tidal volumes.[24] As demonstrated in Fig. 2(h), our method was effective for actuating the movement of liquid plugs and their propagation along the length of the airway channel. Unlike static plugs, the moving liquid plugs showed convex front

menisci and were observed to deposit small amounts of liquid from their trailing edge. The deposited liquid then rapidly wetted the surface despite the intrinsic hydrophobicity of PDMS and formed a thin, continuous liquid lining along the channel walls [Fig. 2(i)]. The increased surface wettability of PDMS observed during this process is presumably due to the altered surface chemistry of PDMS channel walls caused by fibronectin coating and adsorption of soluble factors in the epithelial medium used for submerged culture (Fig. S1). The loss of fluid during the formation of the surface film, however, was not significant enough to induce any measurable changes in the length of moving liquid plugs (Fig. S2). Our flow analysis confirmed the physiological velocity of plug propagation and also revealed that for a given plug length, the speed of plug movement increased in proportion to the flow rate of compressed air [Fig. 2(j)]. For instance, for 2 mm-long liquid plugs, the propagation speed increased linearly from 1.25 to 5.50 mm/s as the air flow rate was raised from 0.03 to 0.1 ml/s. At low flow rates, however, the liquid plugs often halted in the downstream region, rather than propagating through the entire length of the airway channel.

Our microfluidic airway model also provided a platform to simulate unique transport phenomena during the motion of liquid plugs *in vivo*. During inspiration, liquid plugs propagate throughout the complex branching network of the respiratory system consisting of a large number of bifurcating airways. Studies have shown that airway bifurcations affect the dynamics of plug propagation and act as a major determinant of liquid distribution or removal in the lung by inducing splitting of liquid plugs moving through the airway tree.[15,25] This naturally occurring process has also been suggested to affect mechanical stresses and their gradients acting on the airway epithelium generated by plug propagation.[25–27] In our study, we explored the feasibility of modeling this unique physiological transport phenomenon by incorporating a branching channel into the upper layer to create a microchannel bifurcation in the airway compartment [Fig. 2(k)]. When the branching channel was blocked, liquid plugs traveling from the plug generator were initially lodged at the bifurcation but they were released immediately and continued their motion towards the cell culture chamber without any loss of liquid into the branching channel [Fig. 2(l)]. As demonstrated in Fig. 2(m), liquid plugs exhibited a significantly different behavior when the branching channel was open. In this case, continuous airflow through the airway channel pushed the liquid plug lodged at the bifurcating junction evenly to the branching channel and the cell culture chamber. This initial deformation was followed by advancing motion of the front menisci of the plug into both channels. Within a few seconds, this process led to symmetric splitting of the plug and propagation of the resultant daughter plugs towards the downstream of the airway and branching channels. Although our microengineered airway bifurcation differs from the branching geometry of native airways, these results suggest the possibility of leveraging our microengineered model to reconstitute complex and dynamic transport processes involved in the propagation and distribution of liquid plugs in the lungs.

Mechanical injury of the microengineered airway epithelium due to liquid plugs

During microfluidic culture in our device, primary human SAECs seeded on the permeable membrane in the airway channel continuously proliferated and formed a confluent monolayer over the entire membrane surface within 3 days [Fig. 3(a)]. At this point, intimate intercellular contact inhibited further proliferation of the cells. Incubation of the confluent cell population with differentiation medium prior to ALI culture had no adverse effects on the viability and integrity of the epithelium (data not shown). When the medium was aspirated from the airway channel to initiate ALI culture, the monolayer remained intact, and no fluid leakage into the airspace was detected [Fig. 3(b)], indicating structural integrity of the epithelial monolayer produced by submerged culture in our model. ALI culture of SAECs for 5 days resulted in the formation of tight epithelial barrier as evidenced by robust immunostaining of the tight junction protein ZO-1 across the epithelium [Fig. 3(c)]. We also found out that our culture conditions were effective for maintaining the cells viable throughout the culture period, yielding an average viability of 95% at the end of ALI culture.

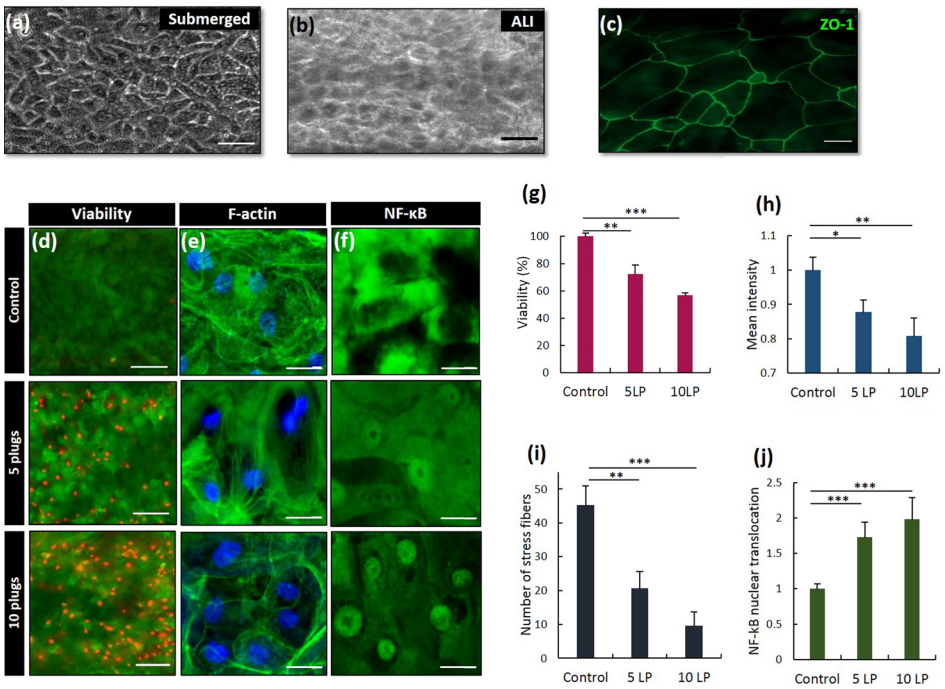

FIG. 3. Biological responses of the microengineered airway epithelium to plug propagation. (a) Primary human SAECs are cultured submerged in medium in the airway channel to form a confluent epithelial monolayer. Scale bar, 200 μm. [(b) and (c)] Subsequent ALI culture for 5 days generates an epithelial barrier that shows tight junctions. Scale bars, 200 μm (phase contact micrograph) and 30 μm (ZO-1 fluorescence micrograph). (d) Plug propagation results in mechanical cell injury in a dose dependent manner. Green and red show live and dead cells, respectively. Scale bars, 100 μm. (e) Cellular injury is accompanied by the disruption of actin cytoskeleton. Increasing the number of passing plugs results in a significant loss of actin filaments in the cytoplasm. Green and blue show F-actin and nuclear staining, respectively. Scale bars, 30 μm. (f) The cells subjected to the propagation of liquid plugs also show activation and nuclear translocation of NF-κB (green). Scale bars, 30 μm. Quantification of (g) cell viability, (h) mean fluorescence intensity of F-actin staining, (i) the number of stress fibers, and (j) nuclear translocation of NF-κB under different loading conditions. Control, 5 LP, and 10 LP represent mechanical stimulation of the cells with airflow, 5 liquid plugs, and 10 liquid plugs, respectively. $^{***}P < 0.001$, $^{**}P < 0.01$, $^{*}P < 0.05$. Data show mean ± SD with $n = 3$.

Once the small airway epithelium was prepared, we then generated the flow of liquid plugs over the apical surface of the cells to simulate and investigate acute cellular responses to plug propagation. Computational models of airway reopening have shown that plug-induced mechanical forces experienced by airway epithelial cells are significantly influenced by the propagation velocity.[13,28] Therefore, special attention was paid to keep the speed of liquid plugs the same at 0.05 ml/min across experiments, and the level of mechanical stresses was varied solely by changing the frequency of plug propagation based on previous reports of plug-induced airway injury.[19,20] First, the epithelium was exposed to 5 passages of liquid plugs at the rate of 1 plug/min. As shown in Fig. 3(d), this condition induced significant irreversible injury of the epithelium, resulting in approximately 30% reduction in cell viability as compared to a control group in which the epithelial cells were exposed to the flow of humidified air at the same speed [Fig. 3(g)]. When the dose of mechanical stimulation was increased to 10 events of plug propagation (1 plug/min), the average cell viability further decreased to roughly 50% [Figs. 3(d) and 3(g)]. These results quantitatively match experimental findings from previous *in vitro* studies[20] and illustrate the deleterious potential of fluid mechanical stresses generated by moving liquid plugs to induce necrotic cell death and airway injury in a dose-dependent manner. It should be noted that our model may overestimate damage of the native tissue as it does not account for the protective effect of endogeneous materials in airway mucus and surface liquid (e.g., surfactant) that have been shown to reduce mechanical forces due to the motion of liquid plugs.[19] Considering that obstructive pulmonary diseases are often associated with the dysfunctional

airway surface liquid,[2–5] however, our system still provides a physiologically relevant model platform to study mechanical injury in diseased human lungs.

Effect of plug propagation on intracellular architecture and pro-inflammatory pathways

While cell viability serves as a good quantitative metric for evaluating tissue injury due to liquid plugs, it fails to capture a variety of other important biological responses triggered by plug propagation that may contribute to the development and progression of pathophysiological conditions. To address this point, we carried out further investigation of epithelial responses to plug flow in our model. For this study, we first examined intracellular architecture of SAECs under different loading conditions through immunohistochemistry-based microfluorimetric analysis of actin cytoskeleton. As illustrated by F-actin staining in Fig. 3(e), the vast majority of cells cultured in the control device displayed a complex network of well-defined actin bundles in their cytoplasm. Mechanical stimulation with the flow of 5 plugs, however, led to a substantial loss of actin filaments and spatial localization of actin staining to cell-cell junctions [middle image, Fig. 3(e)]. These observations were verified by significant reduction in the average intensity of overall actin staining [Fig. 3(h)] and the number of cytoplasmic stress fibers [Fig. 3(i)]. The plug-induced alterations in actin cytoskeleton became more pronounced when the airway epithelium was loaded with a higher level of mechanical stress using 10 plugs driven at the same frequency (1 plug/min) [bottom image, Fig. 3(e)]. These results clearly indicate compromised integrity of intracellular architecture that can be attributed to disrupted homeostasis and structural failure of actin stress fibers due to externally applied acute mechanical perturbations.[29] One possible mechanism of these deleterious cytoskeletal responses is through disorganization and fragmentation of actin filaments due to flow-induced mechanical stresses, which have been previously demonstrated in *in vitro* culture of pulmonary epithelial cells.[30] When the lung experiences frequent airway closure in a chronic manner, the observed cytoskeletal changes may also have adverse longer-term effects on the structural integrity of the airway epithelium and contribute to compromised epithelial barrier function characteristic of many obstructive lung diseases.[29]

Considering that airway inflammation is a common pathophysiological phenotype in a variety of obstructive lung disorders,[5] we also investigated whether mechanical forces produced by moving plugs have the capacity to elicit inflammatory responses in our microengineered airway model. In particular, our study focused on the analysis of NF-κB, which is a transcription factor that regulates the expression of various genes involved in inflammatory and acute stress responses.[31–33] In the control device, immunostaining of NF-κB was confined to the cytoplasm of SAECs, indicating its inactive state[32] [top image, Fig. 3(f)]. After the passage of 5 plugs in the airway channel, the epithelium began to show measurable differences in the intracellular distribution of NF-κB. Most notably, the intensity of immunofluorescence in the nuclear compartment increased significantly while the cytoplasmic level of NF-κB decreased in comparison to the control group [middle image, Fig. 3(f)]. These changes were clearly indicative of activation and subsequent nuclear translocation of NF-κB due to plug propagation.

Doubling the dose of mechanical stress (10 plugs) accentuated this response, and the immunofluorescence of NF-κB was detected predominantly in cell nuclei [bottom image, Fig. 3(f)]. Quantification of our data revealed that as compared to control, exposure of the epithelium to 5 and 10 plugs resulted in 1.7- and 2-fold increases in nuclear translation of NF-κB, respectively [Fig. 3(j)]. These data suggest that the propagation of liquid plugs may induce not only mechanical injury of the epithelium but also significant inflammatory responses. These types of mechanically triggered acute inflammatory responses are often transient and can be resolved over time but repetitive closure of airways in diseased lungs may lead to chronic airway inflammation and the recruitment of inflammatory cells, exacerbating liquid plug-induced airway injury.

CONCLUSION

The formation and propagation of mucus plugs in pulmonary airways represent a unique biotransport phenomenon involved in various aspects of respiratory pathophysiology. Our study described here introduces a novel biomimetic approach to emulating this process in a precisely

controlled experimental model system. By combining this platform with *in vitro* culture of primary human airway cells, this paper demonstrated the capability of our microengineered airway model to screen and quantitatively analyze adverse biological effects of plug propagation. Although our system bears similarities to existing on-chip models of human airways,[15–21] the bioinspired design of a liquid plug demonstrated in this paper makes it a unique and enabling platform for the study of airway closure-induced mechanical lung injury.

To realize the potential of our model as a novel research platform, further studies are necessary to improve its complexity and physiological relevance. For example, airway closure due to mucus plugs is a key characteristic of obstructive pulmonary diseases. Therefore, it would represent a major advance from this study to incorporate primary airway epithelial cells derived from patients with such conditions and to examine how their responses differ from those of normal airway epithelial cells. Engineering the composition of liquid exudates is also necessary to match the physicochemical properties of mucus and airway surface liquid *in vivo* that have a major influence on the level of plug-generated mechanical forces. These types of more physiological liquid plugs may also be used in our platform to realistically model and study the dynamic properties and flow behavior of mucus plugs in the airway system. Considering that plug propagation often leads to the rupture of liquid plugs and subsequent reopening of closed airways,[22] recapitulating the dynamic process of plug rupture may be another important goal of future investigations. The significance of this effort is highlighted by previous findings that mechanical forces due to plug rupture may be more detrimental to the airway epithelium than those produced by plug propagation.[20] Finally, studies are necessary to investigate the scalability of our platform, especially for the purpose of modeling the behavior of liquid plugs at higher levels of organization in the respiratory system. One promising approach to this end is to implement a branching network of microchannels that resembles multiple generations of conducting airways in the lung. The compartmentalized design of our system would also make it possible to vary the position of the underlying hydrogel chambers and thus the location of plug formation within the engineered airway tree. These types of advanced airway models may provide an enabling platform to study more complex transport phenomena involving multiple plugs generated simultaneously in different locations.[34,35]

From the standpoint of developing *in vitro* models, the respiratory system represents an area of significant challenge mainly due to its complex and dynamic mechanical environment. Our work provides a great example of harnessing the power of microengineering and organ-on-a-chip strategies to tackle these challenges and to achieve a new level of sophistication that has not been possible in traditional *in vitro* models. We believe that the novel capabilities for modeling and analysis demonstrated in this paper will pave the way for further development of advanced *in vitro* platforms for basic and translation research into a variety of physiological and pathological processes in the human lung.

SUPPLEMENTARY MATERIAL

See supplementary material for analysis of (i) the surface wettability of PDMS and (ii) plug length during propagation in the microfluidic airway model.

ACKNOWLEDGMENTS

We thank G. Al, M. Mondrinos, and K. W. Kwon for their input and technical assistance. This work was supported by the National Institutes of Health (NIH) (1DP2HL127720-01), the National Science Foundation (CMMI:15-48571), and the University of Pennsylvania. D.H. is a recipient of the NIH Director's New Innovator Award and the Cancer Research Institute Technology Impact Award.

[1]J. E. Scott, S. Y. Yang, E. Stanik, and J. E. Anderson, Am. J. Respir. Cell Mol. Biol. **8**, 258 (1993).
[2]J. C. Hogg, F. Chu, S. Utokaparch, R. Woods, W. M. Elliott, L. Buzatu, R. M. Cherniak, R. M. Rogers, F. C. Sciurba, H. O. Coxson, and P. D. Pare, N. Engl. J. Med. **350**, 2645 (2004).
[3]C. Guérin, S. LeMasson, R. de Varax, J. Milic-Emili, and G. Fournier, Am. J. Respir. Crit. Care Med. **155**, 1949 (1997).
[4]J. C. in't Veen, A. J. Beekman, E. H. Bel, and P. J. Sterk, Am. J. Respir. Crit. Care. Med. **161**, 1902 (2000).

[5]D. Yager, R. D. Kamm, and J. M. Drazen, Chest **107**(3), 105S (1995).
[6]H. Fujioka and J. B. Grotberg, J. Biomech. Eng. **126**, 567 (2004).
[7]D. P. Gaver, D. Halpern, O. E. Jensen, and J. B. Grotberg, J. Fluid Mech. **319**, 25 (1996).
[8]O. E. Jensen, M. K. Horsburgh, D. Halpern, and D. P. Gaver, Phys. Fluids **14**, 443 (2002).
[9]D. Halpern, S. Naire, O. E. Jensen, and D. P. Gaver, J. Fluid Mech. **528**, 53 (2005).
[10]A. M. Jacob and D. P. Gaver, Phys. Fluids **17**, 031502 (2005).
[11]M. Heil, J. Fluid Mech. **424**, 21 (2000).
[12]A. M. Bilek, K. C. Dee, and D. P. Gaver, J. Appl. Physiol. **94**, 770 (2003).
[13]S. S. Kay, A. M. Bilek, K. C. Dee, and D. P. Gaver, J. Appl. Physiol. **97**, 269 (2004).
[14]D. P. Gaver, A. M. Jacob, A. M. Bilek, K. C. Dee, D. Dreyfuss, G. Saumon, and R. D. Hubmayr, *Ventilator-Induced Lung Injury* (Taylor & Francis, New York, 2006), p. 157.
[15]Y. Zheng, H. Fujioka, S. Bian, Y. Torisawa, D. Huh, S. Takayama, and J. B. Grotberg, Phys. Fluids **21**(7), 071903 (2009).
[16]H. Tavana, C. H. Kuo, Q. Y. Lee, B. Mosadegh, D. Huh, P. J. Christensen, J. B. Grotberg, and S. Takayama, Langmuir **26**(5), 3744 (2010).
[17]H. Tavana, D. Huh, J. B. Grotberg, and S. Takayama, Lab. Med. **40**(4), 203 (2009).
[18]A. J. Calderón, Y. S. Heo, D. Huh, N. Futai, S. Takayama, J. B. Fowlkes, and J. L. Bull, Appl. Phys. Lett. **89**(24), 244103 (2006).
[19]H. Tavana, P. Zamankhan, P. J. Christensen, J. B. Grotberg, and S. Takayama, Biomed. Microdevices **13**(4), 731 (2011).
[20]D. Huh, H. Fujioka, Y. C. Tung, N. Futai, R. Paine, J. B. Grotberg, and S. Takayama, PNAS **104**(48), 18886 (2007).
[21]Y. Zheng, H. Fujioka, J. C. Grotberg, and J. B. Grotberg, J. Biomech. Eng. **128**(5), 707 (2006).
[22]J. Seo, D. Conegliano, M. Farrell, M. Cho, X. Ding, T. Seykora, D. Qing, N. S. Mangalmurti, and D. Huh, Sci. Rep. **7**(1), 3413 (2017).
[23]J. B. Grotberg, Annu Rev. Biomed. Eng. **3**, 421 (2001).
[24]H. C. Yalcin, S. F. Perry, and S. N. Ghadiali, J. Appl. Physiol. **103**(5), 1796 (2007).
[25]B. L. Vaughan and J. B. Grotberg, J. Fluid Mech. **793**, 1 (2016).
[26]C. P. Ody, C. N. Baroud, and E. De Langre, J. Colloid Interface Sci. **308**(1), 231 (2007).
[27]Y. Song, M. Baudoin, P. Manneville, and C. N. Baroud, Med. Eng. Phys. **33**(7), 849 (2011).
[28]S. N. Ghadiali and D. P. Gaver, Respir. Physiol. Neurobiol. **163**(1-3), 232 (2008).
[29]M. A. Smith, E. Blankman, M. L. Gardel, L. Luettjohann, C. M. Waterman, and M. C. Beckerle, Dev. Cell **19**(3), 365 (2010).
[30]S. K. Mahto, J. T. Katan, A. Greenblum, B. R. Rutishauser, and J. Sznitman, Am. J. Physiol. Lung. Cell Mol. Physiol. **306**(7), L672 (2014).
[31]T. D. Gilmore, Oncogene **25**(51), 6680 (2006).
[32]M. D. Jacobs and S. C. Harrison, Cell **95**(6), 749 (1998).
[33]A. Kumar and A. M. Boriek, FASEB J. **17**(3), 386 (2003).
[34]M. Baudoin, Y. Song, P. Manneville, and C. N. Baroud, PNAS **110**(3), 859 (2013).
[35]N. V. Quintero, Y. Song, P. Manneville, and C. N. Baroud, Biomicrofluidics **6**(3), 034105 (2012).